Phase-field crystal modeling of nucleation including homogeneous and heterogeneous processes, and growth front nucleation

Gránásy L[1),2)], Podmaniczky F[1)], Tóth GI[1),3)]
1 Wigner Research Centre for Physics, POB 49, 1525 Budapest, Hungary,
granasy.laszlo@wigner.mta.hu, podmaniczky.frigyes@wigner.mta.hu
2 BCAST, Brunel University, Uxbridge, Middlesex, UB8 3PH, United Kingdom,
3 University of Bergen, Allégaten 55, 7005 Bergen, Norway, gyula.toth@ift.uib.no

1. ABSTRACT

Structural aspects of crystal nucleation in undercooled liquids are explored using a nonlinear hydrodynamic theory of freezing proposed recently, which is based on combining fluctuating hydrodynamics with the phase-field crystal (PFC) theory. It will be shown that unlike the usual PFC models of diffusive dynamics, within the hydrodynamic approach not only the homogeneous and heterogeneous nucleation processes are accessible, but also growth front nucleation, which leads to the formation of differently oriented grains at the front in highly undercooled systems. Formation of dislocations at the solid-liquid interface and the interference of density waves ahead of the crystallization front are responsible for the appearance of new orientations.

Key Words: Hydrodynamic theory of freezing, molecular theory, homogeneous nucleation, particle induced crystallization, growth front nucleation, crystallization kinetics.

2. INTRODUCTION

A promising molecular scale method for addressing the structural aspects of solidification is the Phase-Field Crystal (PFC) [1, 2] model. Most of the PFC simulations were done using diffusive dynamics, which corresponds to crystalline aggregation of colloidal particles in suspension. In a recent work, we have proposed a hydrodynamic theory of freezing (HPFC) [3] that starts from fluctuating nonlinear hydrodynamics [4] and employs the free energy functional of the PFC model in determining the reversible stress tensor. The HPFC model recovers the proper dispersion relation for long wavelength acoustic phonons, a *steady state front velocity*, which is inversely proportional to the viscosity (as opposed to the time dependent front velocity observed in diffusive dynamics), and it describes the stress relaxation reasonably [3].

Herein, we employ this HPFC model for describing homogeneous and heterogeneous crystal nucleation, and the formation of new grains at the solidification front. The latter process is termed “growth front nucleation”, and plays an essential role in the formation of spherulites and other polycrystalline growth forms [5, 6].

2.1. Hydrodynamic model of solidification

The momentum transport and continuity equations are written in the form used in fluctuating nonlinear hydrodynamics (FNH) [4]:

$$\frac{\partial \mathbf{p}}{\partial t} + \nabla\cdot(\mathbf{v}\otimes\mathbf{p}) = \nabla\cdot[\mathbf{R}(\rho) + \mathbf{D}(\mathbf{v}) + \mathbf{S}] \quad (1)$$

$$\frac{\partial \rho}{\partial t} + \nabla\cdot\mathbf{p} = 0 \quad (2)$$

where $\mathbf{p}(\mathbf{r}, t)$ is the momentum, $\rho(\mathbf{r}, t)$ the mass density, $\mathbf{v} = \mathbf{p}/\rho$ the velocity, $\nabla\cdot\mathbf{R} = -\rho\nabla\{\delta\Delta F[\rho]/\delta\rho\} \approx -\rho_0\nabla\{\delta\Delta F[\rho]/\delta\rho\}$ is the reversible stress tensor, ρ_0 a reference density, and $\mathbf{D} = \mu_S\{(\nabla\otimes\mathbf{p})+ (\nabla\otimes$

$\mathbf{p})^{\mathrm{T}}\} + [\mu_B - (2/3)\mu_S]\,(\nabla\cdot\mathbf{v})$ the dissipative stress tensor, while **S** is a stochastic momentum noise of correlator

$$\langle S_{ij}(\mathbf{r},t), S_{kl}(\mathbf{r}',t')\rangle = \left(2kT\mu_S\right)\left[\left(\delta_{ik}\delta_{jl} - \delta_{jk}\delta_{il}\right) + \left(\frac{\mu_B}{\mu_S} - \frac{2}{3}\right)\delta_{ij}\delta_{kl}\right]\delta(\mathbf{r}-\mathbf{r}')\delta(t-t'), \qquad (3)$$

where μ_S and μ_B are the shear and bulk viscosities.

In order to avoid violent interatomic flow in the bulk crystal owing to the large density gradients in the hydrodynamic equations, we employ coarse-grained momentum and density fields when computing the velocity field: $\mathbf{v} = \hat{\boldsymbol{p}}/\hat{\rho}$. (See the details in Ref. [3].)

2.2. Materials parameters and numerical solution

Properties of liquid iron as specified in Ref. [3] were used. The melting point is characterized by the reduced temperature $\varepsilon_L = 0.0923$ and the scaled liquid density $\psi_L = -0.1982$ in the usual 2D phase diagram of the PFC model (see Refs. [1, 2] for the latter). The respective linear stability limits taken at constant density or at constant temperature are $\varepsilon_c = 0.1178$ and $\psi_c = -0.1754$, respectively. The reduced temperature, and thus the undercooling, has been tuned by varying the model parameter C_0 of Ref. [3]. The kinetic equations were solved using a pseudo-spectral scheme with a second order Runge–Kutta time stepping, while assuming periodic boundary conditions.

3. RESULTS AND DISCUSSION

3.1. Homogeneous crystal nucleation

The momentum noise present in the momentum equation of FNH gives rise to density fluctuations. This, together with molecular scale density waves emerging from the reversible stress tensor, leads to the formation of crystal-like fluctuations, homogeneous nucleation, followed by crystal growth, and eventually to polycrystalline freezing. Snapshots of this process are shown in Fig. 1, indicating a fairly long incubation period, followed by a rather brief period, in which nucleation and growth occur simultaneously. We fitted the Johnson-Mehl-Avrami-Kolmogorov expression, $X(t) = 1 - \exp\{-[(t - t_0)/\tau]^p\}$ [5], to the temperature dependent crystalline fraction evaluated from the molecular density. Here t_0 is the incubation time, τ a characteristic time related to the nucleation and growth rates, and p the Avrami-Kolmogorov exponent regarded indicative of the mechanism of crystallization [5]. In our case, from the local slope of the $\ln\{-\ln(1-X)\}$ vs. $\ln(t - t_0)$ plot, we obtained a p that increases between 3 and 4 roughly linearly with increasing crystalline fraction, a behavior that might be associated with increasing nucleation rate, which in turn would imply that during the short solidification time steady state nucleation rate was not established.

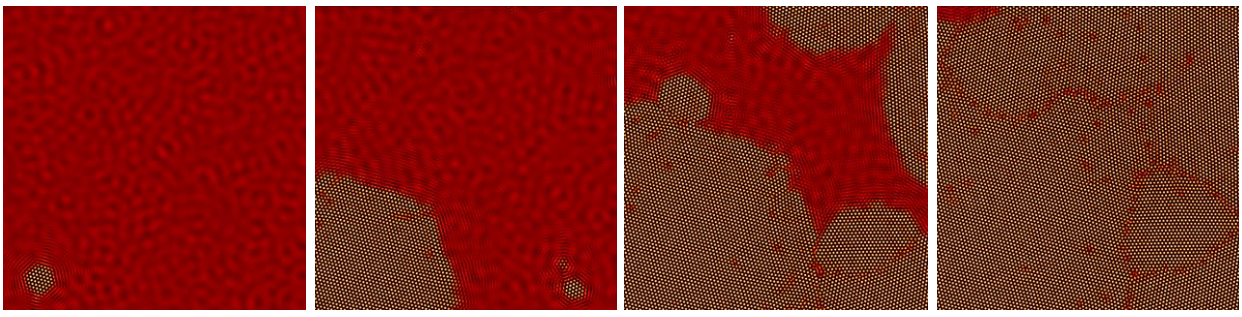

Fig. 1: Snapshots of (homogeneous) crystal nucleation and growth in the HPFC model, at dimensionless times t = 3800, 4500, 5000, and 5500. (600^2 sections of 2048^2 images are shown.) The reduced temperature is $\varepsilon = 0.1158$, obtained using $0.975C_0$ (the liquid is near its stability limit, yet still in the metastable regime). The density fluctuations in the liquid emerge from the momentum fluctuations, while molecular scale density waves can be observed at the crystal-liquid interface.

3.2. Particle induced crystallization

To model a crystalline substrate, we added an extra term, $V(\mathbf{r})\rho(\mathbf{r}, t)$, to the free energy density, where $V(\mathbf{r}) = 0$ outside the domain of the substrate, whereas it is a periodic potential inside that determines the crystal lattice of the substrate. Here a square lattice is used, whose lattice constant coincides with that of the equilibrium triangular crystal, enabling a nearly ideal wetting of the substrate by the crystal. The linear size of the substrate we used was 32 lattice constants. We explore, whether the free growth limited model of Greer *et al.* [6] remains valid in the presence of hydrodynamics. The undercooling has been increased by multiplying the model parameter C_0 by factors, 0.999, 0.998, 0.995, and 0.990. In Fig. 2, we present long-time solutions as a function of C_0. It is found that, as suggested in Ref. [6], for a given particle size, there exists a critical undercooling, beyond which free growth takes place.

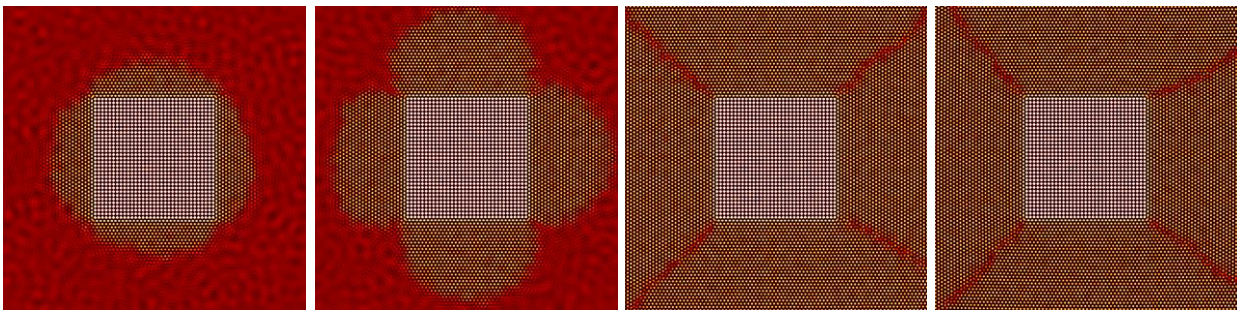

Fig. 2: Snapshots of simulations ($t = 2\times10^4$, 1.2×10^4, 10^4, and 10^4) for particle induced crystallization in the HPFC model. The undercooling increases from left to right: 0.999 C_0, 0.998 C_0, 0.995 C_0, and 0.990 C_0 were used. (600^2 sections of 2048^2 images are shown. The light square at the center is the substrate.) On the left stable configurations are displayed, while those on the right grow.

3.3. Growth front nucleation

Growth Front Nucleation (GFN): formation of new grains at the propagating solidification front has been identified as the mechanism by which complex polycrystalline growth forms appear [7, 8]. This phenomenon has been successfully modeled by phase-field methods relying on an orientation field that describes the local crystallographic orientation. In this approach, the formation of new grains happens either by quenching orientational defects (bundles dislocations) into the crystal, or via branching in the directions of low grain-boundary energies. This approach, relying on coarse grained fields, became fairly successful in capturing rather complex structures [7 – 9]. Yet it is desirable to clarify the microscopic background of GFN. Here, we address the formation of new grains at the solid-liquid interface at high undercoolings within the framework of the HPFC model.

We made our first attempts to model GFN on the molecular scale years ago using the original PFC model relying on diffusive dynamics. At supersaturations beyond the linear stability regime of the liquid [$\psi_c = -(\varepsilon/3)^{1/2}$] without noise, we observed that crystal seeds developed into ordered polycrystalline structures. Beyond the stability limit, the growing crystal was surrounded by concentric density waves, which initiated crystallization accordingly: in six directions these waves helped the growth of the original crystal, whereas in other directions a large number of defects formed and new orientations appeared that fitted better to the local direction of the density waves. This could be viewed as an elementary process of GFN. Unfortunately, in this regime the liquid is unstable: when noise is added to the respective equation of motion, this phenomenon is suppressed by explosive crystallization. Inside the metastable regime, owing to the lack of such density waves, we were unable to observe the GFN phenomenon.

In the case of the HPFC model, we were more successful. We were able to grow polycrystalline domains at a large undercooling as illustrated in Fig. 3. The kinetic equations were solved on a 2024^2 rectangular grid. To analyze the local structure, we used a complex order parameter, $g_6 = \sum_j \exp\{-6i\theta_j\}$, where summation is for the nearest neighbors, and θ_j is the angle of the vector pointing to the j^{th} neighbor in the laboratory frame. The magnitude of g_6 represents the degree of order in the neighborhood, whereas its phase shows the local orientation.

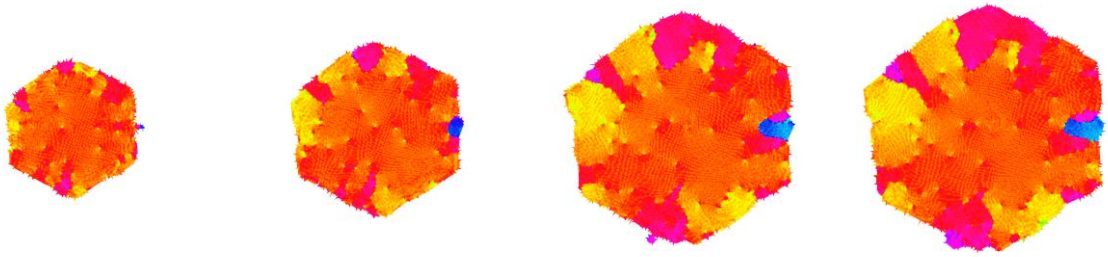

Fig. 3: Growth front nucleation (GFN) in the HPFC model at a large undercooling, yet in the metastable liquid regime (0.975 C_0 was used as in Fig 1). Different colors stand for different crystallographic orientations. Snapshots of the orientation field were taken at dimensionless times, t = 2100, 2600, and 3400, before homogeneous nucleation sets in.)

Fig. 3 shows the evolution of the orientation field. The simulation was performed in a regime, where the liquid is metastable with respect to fluctuations. A shallow molecular size potential well was used to initiate freezing. It induces concentric density waves, then a crystal forms, which grows as a single crystal, but gradually new orientations appear via two mechanisms of GFN: (1) Dislocations enter at the corners and at the center of the edges of the hexagonal crystal. These can be misfit dislocations, emerging from the stress field of the growing nanoscale crystallite. (2) Small crystallites nucleate in the close vicinity of the solid-liquid interface, which apparently originate from the interference of the density waves emanating from the rough solid-liquid interface. (Note the small protrusions on the right and lower left sides of the crystal in the 1st and 3rd panels, from which the blue and magenta grains grow.) Work is underway to quantify these phenomena in detail.

Finally, it remains an intriguing question why the HPFC model recovers GFN at large driving forces, whereas the PFC model relying on diffusive dynamics does not. A possible explanation is that, in the latter case, a fast growth mode characterized by a broad interface occurs at large driving forces [10], in which healing of the defects can be relatively easy, avoiding thus the formation of dislocations at the perimeter of the growing crystal, preventing thus GFN.

This work has been supported by the EU FP7 Collaborative Project “EXOMET” (contract no. NMP-LA-2012-280421, co-funded by ESA).

REFERENCES

1. K. R. Elder, M. Katakowski, M. Haataja, M. Grant, Phys. Rev. Lett. **88**, 2002, 245701-1-4.

2. For review see: H. Emmerich, H. Löwen, R. Wittkowski, T, Gruhn, G. I. Tóth, G. Tegze, L. Gránásy, Adv. Phys. **61**, 2012, 665-743.

3. G. I. Tóth, L. Gránásy, G. Tegze, J. Phys.: Condens. Matter **26**, 2014, 055001.

4. B. Z. Shang, N. K. Voulgarakis, J.-W. Chu, J. Chem. Phys. **135**, 2011, 044111.

5. J. W. Christian, *Transformations in Metals and Alloys*, Pergamon, Oxford, 1981.

6. A. L. Greer, A.M. Brunn, A. Tronche, P.V. Evans, D. J. Bristow, Acta Mater. **48**, 2000, 2823-2835.

7. L. Gránásy, T. Pusztai, T. Börzsönyi, J. A. Warren, J. F. Douglas, Nature Mater. **3**, 2004, 645-650.

8. L. Gránásy, L. Rátkai, A. Szállás, B. Korbuly, G. I. Tóth, L. Környei, T. Pusztai, Metall. Mater. Trans. A **45**, 2014, 1694-1719.

9. L. Gránásy, T. Pusztai, G. Tegze, J. A. Warren, J. F. Douglas, Phys. Rev. E **72**, 2005, 011605.

10. G. Tegze, G. I. Tóth, L. Gránásy, Phys. Rev. Lett. **106**, 2011, 195502.